

Characteristics of an Improved Coil Structure for the Magnetic Stereotaxis System

Ye Bai, *Student Member, IEEE*, Qiuliang Wang, Ming Yang, Yunjia Yu, Hongwei Liu, and Keeman Kim

Abstract—The Magnetic Stereotaxis System (MSS) is a unique medical device designed to deliver drugs and other therapies directly into deep brain tissues. This approach uses superconducting coils to manipulate a small permanent magnet pellet attached to a catheter through the brain tissues. The movement of the small pellet is controlled by a remote computer and displayed on a fluoroscopic imaging system. The magnets of the previous generations were composed of three pairs of orthogonal superconducting solenoid coils. The control strategies are complex because of the magnetic field distribution of solenoids. The high inductance values of solenoid coils can severely slow down the ratio of current change and therefore do harm to the control precision of a magnet pellet. This paper presents a novel type of spherical coils that can generate linear gradient fields over a large spherical volume. This type of modified spherical coils with a constant current distribution model is easy to fabricate in engineering and manufacture. A prototype of this spherical magnet has already been constructed with copper conductors at the Applied Superconductivity Laboratory, CAS. We have also completed the design of superconducting spherical coils with NbTi conductors. Simulation and test results of this magnet are also presented.

Index Terms—Linear gradient field, magnetic stereotaxis system, modified spherical coils, quadrupole magnet, $\sin 2\theta$ coils.

I. INTRODUCTION

THE Magnetic Stereotaxis System [1] is a novel neurosurgical tool developed to allow surgical treatment inaccessible regions in the brain by providing minimum damage via a nonlinear approach. The MSS originated from the hopes that a less-invasive methodology could be developed that would allow neurosurgeons to operate in previously inaccessible regions of the brain. By introducing a small permanent magnet pellet into the brain through a small “burr hole” drilled into the skull prior to the operation, large superconducting coils could be used in conjunction with a pushing mechanism to magnetically guide the pellet and an overlaying catheter through the brain’s parenchyma while avoiding the important structures of the brain. The operational methodology of the MSS is expected to be less destructive to the tissues of the brain than the shunts, straight tubes and other devices associated with conventional techniques in neurosurgery.

The first MSS was developed in 1984 as the Video Tumor Fighter [2], a system specifically focused on the eradication

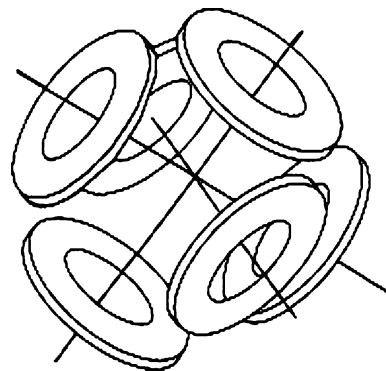


Fig. 1. Three dimensional representation of the coils layout in the recent six-solenoid MSS.

of deep-seated brain tumors via hyperthermia-based treatment. Further studies revealed that the reality of a magneto-motive based system used to direct a small implant promised other numerous applications that include biopsy, delivery of precision radiation or chemicals therapy etc. It was in the light of these possible broadened applications of the VTF that the system became known as the MSS.

Another previous effort in magnetic stereotaxis used a single moveable coil to act upon the implant pellet [3]. This arrangement was proved to be successful in experiments using live dogs. It was difficult to use this device on humans for the size and weight of the required coils interfere with the necessary bi-planar fluoroscopes and make precision manipulation impractical in an operating environment.

Subsequent efforts have focused upon the arrangement of stationary coils [4]. The recent MSS was composed of three pairs of orthogonal superconducting solenoid coils. The arrangement of the six-solenoid is shown in Fig. 1. The superconducting six-solenoid MSS has already been constructed in Virginia.

II. MAGNETIC FIELD ANALYSIS OF MSS

Though both the permanent magnet pellet and soft iron pellet can be used as the implant seed, they show different features in the magnetic field. This paper only discusses the situation of using the permanent magnet pellet.

Because the dimensions of the pellet are very small compared to the size of the superconducting coils, the pellet can be considered as a point magnetic dipole. The magnetic properties of the pellet are summarized by the pellet’s dipole moment m . The direction of this magnetic moment is the same as the direction of the magnetization in the pellet. From the reference [5], we

Manuscript received October 4, 2004.

Y. Bai is with the Institute of Electrical Engineering Chinese Academy of Sciences and with the Graduate School of CAS, Beijing CO 100080, China (e-mail: byeah@mail.iee.ac.cn).

Q. Wang, M. Yang, Y. Yu, and H. Liu are with the Institute of Electrical Engineering Chinese Academy of Sciences, Beijing CO 100080, China.

K. Kim is with Korea Basic Science Institute, Taejon, Korea.

Digital Object Identifier 10.1109/TASC.2005.849662

can derive the force and torque on a magnetic dipole due to an applied magnetic flux density \mathbf{B} . The force on the seed is:

$$\mathbf{F} = \nabla(\mathbf{m} \cdot \mathbf{B}) \quad (1)$$

and the torque is:

$$\mathbf{T} = \mathbf{m} \times \mathbf{B} \quad (2)$$

The Nd-Fe-B permanent magnet pellet has nearly constant magnetic moment \mathbf{m} under a wide range of magnetic field. Thus we can focus our attention to the calculation of field partial derivations. The moment \mathbf{m} is not a function of position vector and the pellet is located in a source-free region. We can obtain the following relationships in Cartesian coordinates:

$$\begin{aligned} \mathbf{F} &= (\mathbf{m} \cdot \nabla) \mathbf{B} \\ &= \left(m_x \frac{\partial}{\partial x} + m_y \frac{\partial}{\partial y} + m_z \frac{\partial}{\partial z} \right) (B_x \mathbf{e}_x + B_y \mathbf{e}_y + B_z \mathbf{e}_z) \\ &= (m_x \ m_y \ m_z) \begin{pmatrix} \frac{\partial B_x}{\partial x} \\ \frac{\partial B_x}{\partial y} \\ \frac{\partial B_x}{\partial z} \end{pmatrix} \mathbf{e}_x + (m_x \ m_y \ m_z) \begin{pmatrix} \frac{\partial B_y}{\partial x} \\ \frac{\partial B_y}{\partial y} \\ \frac{\partial B_y}{\partial z} \end{pmatrix} \mathbf{e}_y \\ &\quad + (m_x \ m_y \ m_z) \begin{pmatrix} \frac{\partial B_z}{\partial x} \\ \frac{\partial B_z}{\partial y} \\ \frac{\partial B_z}{\partial z} \end{pmatrix} \mathbf{e}_z \end{aligned} \quad (3)$$

The subscript x , y and z denote the three orthogonal components of vector \mathbf{B} and \mathbf{m} . \mathbf{e}_x , \mathbf{e}_y and \mathbf{e}_z denote the three unit vectors in Cartesian coordinates.

To guide the small pellet through the brain's parenchyma precisely, it is necessary to calculate the three magnetic flux density components and their spatial partial derivations. For solenoids, this calculation is usually done in cylindrical coordinates since the φ -component of the field vanishes and the other components are φ independent. In cylindrical coordinates the magnetic field has both ρ and z direction components only. In order to translate these calculation results from cylindrical coordinates to Cartesian coordinates, the complex tensor transformations can be used [6]. Since the magnetic flux density distribution of solenoid shown in Fig. 2 is irregular and difficult to map, the partial derivatives of the magnetic field in (3) are difficult to calculate. Although the solenoid coils are convenient to construct, they have the disadvantage of complex field distribution and high levels of the dissipated magnetic energies. The high values of inductances in solenoid coils may prohibit their use in some situations where the current will change frequently. The high values of inductances of solenoid may slow down the ratio of current change and thus is harmful to the control precision in MSS. Moreover, the heavy calculation burden of solving the partial derivatives in (3) will reduce the efficiency of the whole system. In order to guide the pellet precisely and promptly according to its position, a type of new coils with lower inductance values and simpler calculation processes than in solenoids is needed.

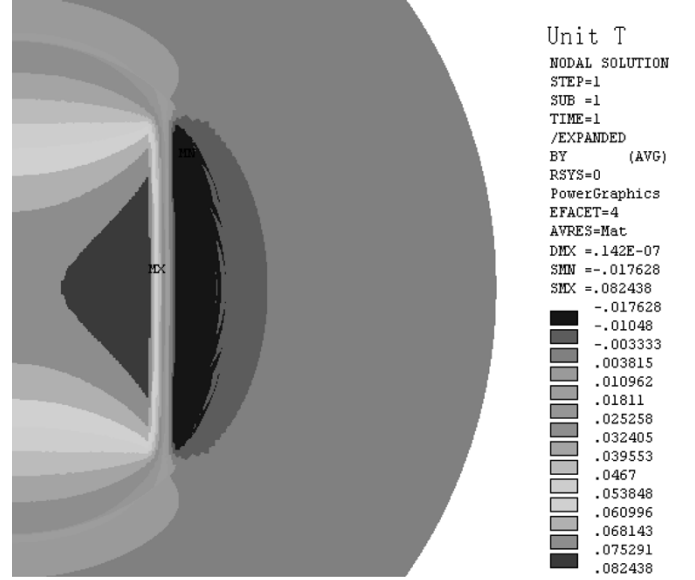


Fig. 2. Distribution of y -component of the magnetic flux density in the solenoid coils.

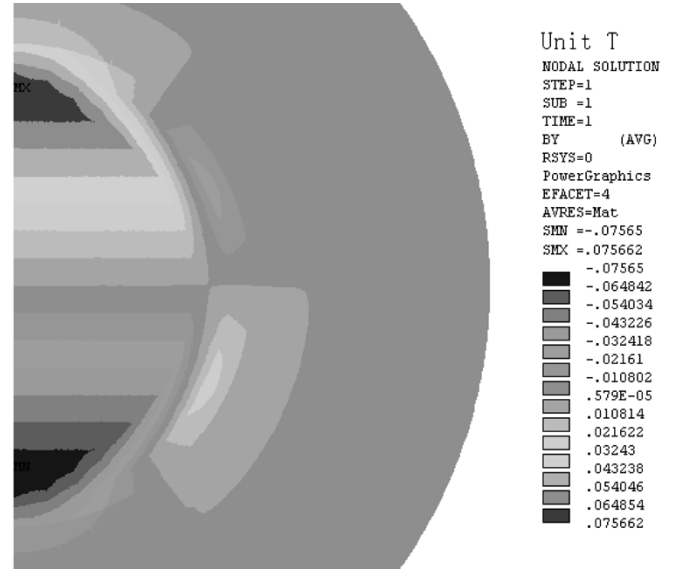


Fig. 3. Distribution of y -component of the magnetic flux density in the spherical coils.

III. A TYPE OF MODIFIED SPHERICAL COILS FOR THE MSS

This paper presents a novel type of modified spherical coils that can generate higher linear gradient fields over a large spherical volume together with lower inductances than the solenoid coils of the same dimensions.

Fig. 2 and Fig. 3 show the distributions of the y -component of the magnetic flux density in solenoid coils and spherical coils of the similar dimensions and current densities. Only the right side of the symmetry axis is shown. Applying the current density $J_0 \sin 2\theta$ along the φ direction in spherical coordinates [7] can generate a linear gradient field inside the sphere. It can be seen clearly that the solenoid coils have a more irregular field distribution than spherical coils. Furthermore, the gradient of spherical coils is higher than that of solenoid coils while the inductance values keep lower. The detailed comparison data are

TABLE I
MAIN PARAMETERS OF SOLENOID COILS AND SPHERICAL COILS

Parameter	Solenoid coils	Spherical coils with $\sin 2\theta$ structure	Modified spherical coils
Inner diameter (mm)	200	200	200
Outer diameter (mm)	240	240	240
Coils height (mm)	240	240	240
Total Ampere-turns (A.t)	768	698	736
Coil current density J_0 (A/mm ²)	4	4	4
Distribution of current density J_φ	J_0	$J_0 \sin 2\theta$	J_0 Angular Extension
Maximum field gradient (T/m)	0.412	0.733	0.810
Inductance values (H)	0.076	0.021	0.024
Linear gradient	No	Yes	Yes
Filling factor	0.785	0.785	0.785

listed in Table I. From the simulation results, it is shown that the spherical coils are more appropriate for the application of MSS.

In the case of spherical coils mentioned above, the current density is confined to lie on the surface of the sphere and is directed along the φ direction. In order to generate the linear gradient field, the spherical coils must have the $\sin 2\theta$ structure, which means the current density values J_φ must vary along the θ direction as shown in Fig. 4(a). This type of $\sin 2\theta$ coils is difficult to construct in engineering and manufacture.

This paper presents a modified spherical coils structure with a constant current density over an angular extension about 60° with quadrupolar symmetry as shown in Fig. 4(b). The simulation results of this type of spherical coils are shown in Fig. 5 and for succinctness only a semi sphere is sufficient.

Using the method of separation of variables [8], [9], the nonzero flux density inside the sphere can be represented as:

$$B_y(r, \theta, \varphi) = \int_{\theta_1}^{\theta_2} \int_{r_0}^{r_1} \frac{\mu_0 J_\varphi}{2} \sum_{n=0}^{\infty} \left(\frac{r}{r_0}\right)^n (n+1) P_n(\cos \theta) \times [P_n(\cos \alpha) - \cos \alpha P_{n+1}(\cos \alpha)] d\alpha dr \quad (4)$$

$$B_x(r, \theta, \varphi) = \int_{\theta_1}^{\theta_2} \int_{r_0}^{r_1} \frac{\mu_0 J_\varphi}{2} \sum_{n=0}^{\infty} \left(\frac{r}{r_0}\right)^n \frac{(n+1)}{\sin \theta} \times [P_{n+1}(\cos \theta) - \cos \theta P_n(\cos \theta)] \times [P_n(\cos \alpha) - \cos \alpha P_{n+1}(\cos \alpha)] d\alpha dr \quad (5)$$

Where $P_n(\cos \theta)$ stands the associated Legendre function, r_0 and r_1 denote the inner and outer radii of the sphere, θ_1 and θ_2 denote the angular extension range. r , θ , and φ denote the three directional components in spherical coordinates and n an integer in the above equations.

Substituting $J_\varphi = J_0 \sin 2\theta$; $\theta_1 = 0$; $\theta_2 = 90$ into (4) and (5), it can get:

$$B_y = \frac{4}{5} \mu_0 J_0 \ln \left(\frac{r_1}{r_0}\right) y$$

$$B_x = -\frac{2}{5} \mu_0 J_0 \ln \left(\frac{r_1}{r_0}\right) x$$

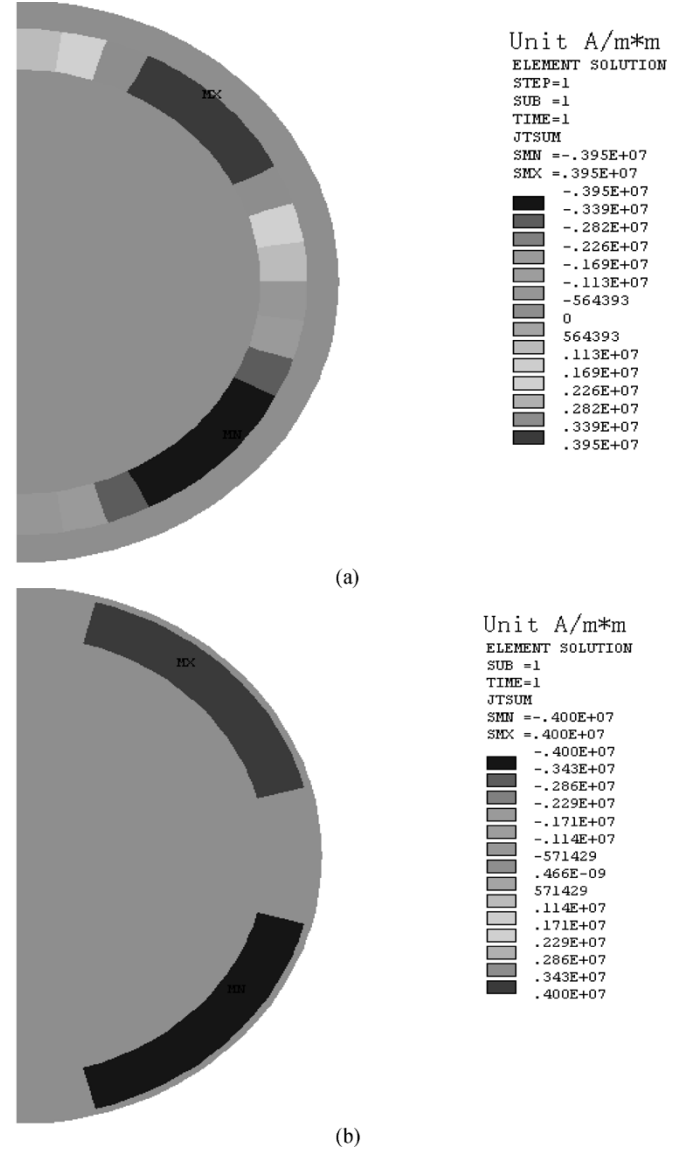


Fig. 4. Distribution of current density. (a) Spherical coils with $J_0 \sin 2\theta$ current density. (b) Modified spherical coils with constant current density.

Substituting $J_\varphi = J_0$; $\theta_1 = 15$; $\theta_2 = 75$ into (4) and (5), it can get the following approximating results:

$$B_y = 0.8838 \mu_0 J_0 \ln \left(\frac{r_1}{r_0}\right) y$$

$$B_x = -0.4419 \mu_0 J_0 \ln \left(\frac{r_1}{r_0}\right) x$$

From the above conclusions it can be seen that the field partial derivatives are much easier to calculate in this modified spherical coils than in solenoid coils. Moreover, $\partial B_x / \partial x$ and $\partial B_y / \partial y$ have constant values in large volumes inside the sphere.

IV. TEST RESULTS

As the first step and in order to verify the finite element calculation results [10], copper conductors are used instead of superconducting conductors to fabricate these spherical coils.

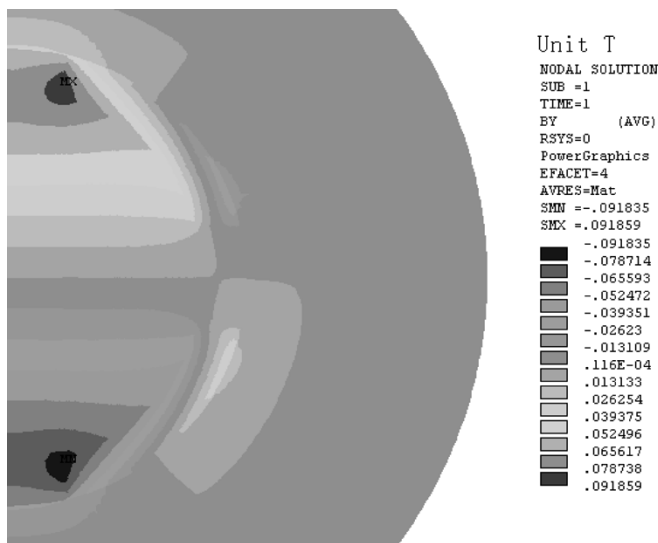


Fig. 5. Distribution of y-component of the magnetic flux density in the modified spherical coils.

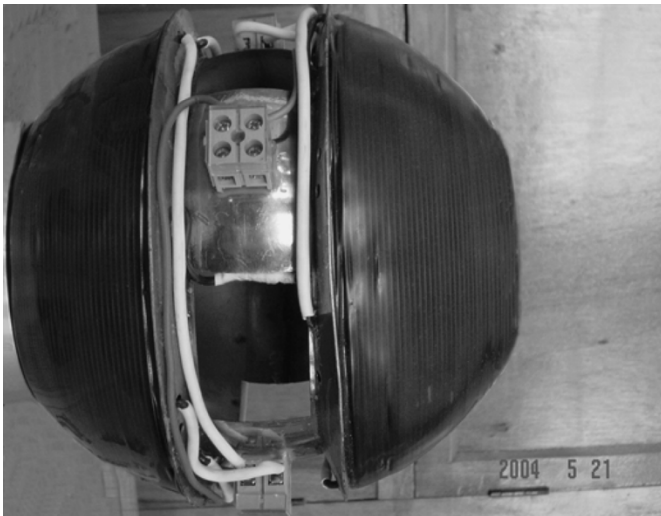


Fig. 6. Photograph of the modified spherical coils.

Prototypes of these modified spherical coils have been constructed as copper shown in Fig. 6. The construction procedures with copper conductors are similar to that with superconducting conductors. Table II lists the measured results of magnetic flux density in the spherical coils with the simulation results. We only measure a few key points inside of the sphere. There are some minor deviations from the theoretical values due to fabrication errors. The current density in the spherical coils is only 1 A/mm^2 to avoid overheating of the copper coils. This coil structure is used for the benefits of smaller magnetic multipole components, simpler construction procedures and relatively higher linear gradient field.

We have also completed the design of superconducting spherical coils. A new superconducting magnet for the MSS will be constructed in the next few months.

TABLE II
VALUES OF MAGNETIC FLUX DENSITY IN MODIFIED SPHERICAL COILS

Measured key points (x, y) (mm)	Calculated (G)	Actual (G)
(0, 10)	20.2	19.4
(0, 20)	40.4	38.9
(0, 30)	60.6	58.3
(0, 40)	80.8	77.8
(0, 50)	110	97.3
(0, 122.5)	136.5	132.8
(10, 0)	10.1	10.9
(20, 0)	20.2	21.9
(30, 0)	30.3	32.8
(40, 0)	40.4	43.7
(50, 0)	50.5	54.9
(122.5, 0)	65.3	62.8

$$G = \text{gauss}, 1T=10^4 G$$

V. CONCLUSION

Two different types of spherical coils have been designed to generate the linear gradient field for the MSS. Compared with the traditional solenoid coils, the spherical coils can generate higher linear gradient field while the inductance values are lower, which is essential for the MSS. In addition, the relatively more succinct expressions of magnetic field partial derivatives will greatly improve the calculation efficiency. Though the modified structure will bring some multipole field components, it is more economic to construct in engineering. The measured fields and gradients agree with the simulation results within the measurement accuracy. Because this new magnet can generate nearly linear gradient field, it may be used as a quadrupole magnet [11], which has widely applications in Fusion research, high-energy physics, particle accelerators, space detectors etc.

REFERENCES

- [1] D. C. Meeker, E. H. Maslen, and R. C. Ritter, "Optimal realization of arbitrary force in a magnetic stereotaxis system," *IEEE Trans. Magn.*, vol. 32, no. 2, pp. 320–327, Mar. 1996.
- [2] M. A. Howard III, R. C. Ritter, and M. S. Grady, "Video tumor fighting system," U.S. Patent 4 869 247, Sep. 26, 1989.
- [3] E. G. Quate, K. G. Wika, and M. A. Lawson, "Goniometric motion controller for the superconducting coil in a magnetic stereotaxis system," *IEEE Trans. Biomed. Eng.*, vol. 38, no. 9, pp. 899–905, Sep. 1991.
- [4] R. G. McNeil, R. C. Ritter, B. Wang, and M. A. Lawson, "Functional design features and initial performance characteristics of a magnetic-implant guidance system for stereotactic neurosurgery," *IEEE Trans. Biomed. Eng.*, vol. 42, no. 8, pp. 793–801, Aug. 1995.
- [5] R. S. Elliot, *Electromagnetic*. New York: McGraw-Hill, 1966.
- [6] I. Sokolnikoff, *Tensor Analysis*. New York: Wiley, 1964.
- [7] Y. Bai, Q. Wang, and Y. Yu, "Target field approach for spherical coordinates," *IEEE Trans. Appl. Supercond.*, vol. 14, no. 2, pp. 1317–1321, Jun. 2004.
- [8] M. Abramowitz and I. Stegun, *Handbook of Mathematical Functions*. Washington: National Bureau of Standards. New York: Dover, 1968 (reprinted).
- [9] Y. Bai, Q. Wang, and Y. Yu, "An approach to spherical coils design based on the target field approach," in *Proc. CSEE*, vol. 24, Jun. 2004, pp. 132–136.
- [10] *ANSOFT User's Manuals and Procedures Guides Revision 7.0*, Ansoft Inc., Pittsburgh, PA, 1998.
- [11] M. S. Livingston and J. P. Blewett, *Particle Accelerators*. New York: McGraw-Hill, 1962.